

Finite-time scaling of dynamic quantum criticality

Shuai Yin,* Xizhou Qin, Chaohong Lee,[†] and Fan Zhong[‡]

State Key Laboratory of Optoelectronic Materials and Technologies, School of Physics and Engineering, Sun Yat-sen University, Guangzhou 510275, People's Republic of China

We develop a theory of finite-time scaling for dynamic quantum criticality by considering the competition among an external time scale, an intrinsic reaction time scale and an imaginary time scale arising respectively from an external driving field, the fluctuations of the competing orders and thermal fluctuations. Through a successful application in determining the critical properties at zero temperature and the solution of real-time Lindblad master equation near a quantum critical point at nonzero temperatures, we show that finite-time scaling offers not only an amenable and systematic approach to detect the dynamic critical properties, but also a unified framework to understand and explore nonequilibrium dynamics of quantum criticality, which shows specificities for open systems.

PACS numbers: 64.70.Tg, 64.60.Ht, 75.10.Pq

Detecting quantum phase transitions (QPTs) and understanding their real-time dynamics are of great importance [1–5]. Recent experimental breakthrough in ultracold atoms [6] promises new tools to study the quantum critical dynamics [7]. In the nonequilibrium critical dynamics of QPTs at zero temperature in which a controlling parameter is changed with time through a critical point [4, 5], the Kibble-Zurek mechanism (KZM), which was first introduced in cosmology by Kibble [8] and then in condensed matter physics by Zurek [9], has been found to describe the dynamics of QPTs well [4, 5, 10]. In this adiabatic–impulse–adiabatic approximation of the KZM, the system considered is assumed to cease evolving in the impulse regime within which adiabaticity breaks down due to critical slowing down [11]. Yet, dynamical scaling has been reported just within this regime [12] and confirmed in both integrable and nonintegrable systems [13, 14]. In classical critical dynamics, an explanation based on coarsening has been developed [15], however in quantum phase transitions, a systematic understanding of the full scaling behavior is still lacking.

On the other hand, natural systems and their measurements exist inevitably in nonzero temperatures, though probably only initial thermal states need considering in ultracold atoms [16]. Thermal effects on a quantum critical state can give rise to a variety of exotic behavior in the famous quantum critical regime (QCR) [17] as exhibits in a wide range of strongly correlated systems [1–3, 18]. Yet, as both phases exhibit complex long-range quantum entanglement near the quantum critical point and are violently excited thermally, it is a great challenge to describe quantum critical dynamics at finite temperatures, let alone nonequilibrium real-time effects [19, 20]. Indeed, none of the analytic, semiclassical, or numerical methods of condensed-matter physics yields accurate results for dynamics in the QCR except for some special systems in 1D [3]. Even in isolated situations it is difficult to study the time evolution of nonequilibrium systems with many degrees of freedom [4, 5, 22–24]. Therefore, systematic approaches have to be invoked.

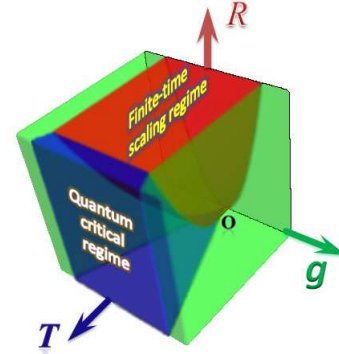


FIG. 1: (color online) Schematic phase diagram under a sweep of g near its critical value 0. Two equilibrium phases (light grey/green) dominated by the reaction time τ_s are separated by two crossover domains fanning out from the quantum critical point O . One domain is the QCR (dark/blue) controlled by the imaginary time scale τ_T . The other is the new FTS (grey/red) regime governed by the driving time scale τ_d .

Time plays a fundamental role in quantum criticality owing to the interplay of static and dynamic behaviors. Specifically, by varying the distance to the critical point g at a time rate R , a continuous QPT at a finite temperature T is characterized mainly by three time scales. The first one is a reaction time τ_s that arises from the fluctuations of the competing orders and blows up as $\tau_s \sim |g|^{-\nu z}$ with the standard critical exponents ν and z as g vanishes [1]. The second one is an “imaginary” time scale $\tau_T = 1/T$ (the Planck and the Boltzmann constants have been set to 1) due to the finite T , since the real time is its analytical continuation to imaginary numbers through a Feynman path integral representation [1]. The third one is an externally imposed driving time scale τ_d that results from the driving and grows as $\tau_d \sim R^{-z/r}$ with a rate exponent r that is related to z and other static critical exponents [25]. It is the competition among τ_s , τ_T , and τ_d that lead to a diversity of equilibrium and dynamic universal phenomena near a quantum critical point.

Here we study systematically the competition among the three characteristic time scales according to the theory of finite-time scaling (FTS) [25]. As seen in Fig. 1, besides the usual equilibrium regimes and the QCR which are respectively dominated by τ_s and τ_T , our most important result is that a new nonequilibrium FTS domain is created. In this domain, τ_d is the shortest time among the trio and thus dominates, just as the well-known regime of finite-size scaling in which the characteristic size L of the system is shorter than its correlation length. At $T = 0$, this indicates the FTS domain overlaps just the impulse regime of the KZM for sweeping g . As a consequence, although the system falls out of equilibrium, the state does not cease evolving; rather, it evolves according to the imposed time scale τ_d instead of τ_s with nonadiabatic excitations obeying FTS. Therefore, FTS improves the understanding of KZM on its dark impulse regime and produces naturally scaling forms suggested in [12–14]. In addition, FTS enables us to study within the same framework other driving dynamics than the KZ protocols [20], which focus on changing non-symmetry breaking terms like g . We shall show that this provides a convenient method to determine the critical points and exponents, which were invoked as input for scaling collapses reported in [12–14]. Similarly, at $T \neq 0$, in the FTS regime, there are now nonadiabatic thermal excitations controlled again by τ_d and thus obeying again FTS. Further, from Fig. 1, the FTS regime pushes the QCR to higher temperatures since only then τ_T dominates. Consequently, FTS enables one to probe directly the quantum critical point and its scaling behavior at nonzero temperatures as T becomes subordinate and just a perturbation. Thus, it shows a ‘dynamic cooling’ effect that enables one to probe the zero-temperature scaling at nonzero-temperatures while keeping T subsidiary. This offers us an extra approach to detect and study quantum criticality at finite temperatures. Owing to its conceptual simplicity and accessibility, FTS therefore provides a unified framework not only to detect the dynamic critical properties, but also to understand and explore the nonequilibrium dynamics of quantum criticality both at $T = 0$ and $T \neq 0$.

As another important result, we shall show that in nonequilibrium quantum critical dynamics of open systems one must include an additional variable such as the coupling to a heat bath to the intrinsic quantum dynamics [21]. This is an important difference from the classical case and must be considered when extending nonequilibrium quantum critical dynamics to finite temperatures [19]. We shall see that the master equation in the Lindblad form just offers such a variable and is thus an appropriate platform to study real-time nonequilibrium quantum criticality.

We start with an open many-body quantum system interacting with a heat bath [19] to study the interplay of quantum and thermal fluctuations. The state of such

a system can be described by a density matrix operator ρ according to quantum statistical physics. For weak system-environment couplings, after assuming Markovian and tracing over the bath variables, one obtains the master equation for ρ in the Lindblad form [26–28],

$$\partial\rho/\partial t = -i[\mathcal{H}, \rho] + c\mathcal{L}\rho, \quad (1)$$

where $\mathcal{L}\rho = -\sum_{i=1, j \neq i}^{N_E} \beta_j (V_{i \rightarrow j}^\dagger V_{i \rightarrow j} \rho + \rho V_{i \rightarrow j}^\dagger V_{i \rightarrow j} - 2V_{i \rightarrow j} \rho V_{i \rightarrow j}^\dagger)/2$, c is the dissipation rate and measures the coupling strength between the system and the bath, N_E is the total number of energy levels, $\beta_i = \exp(-E_i/T)/\text{Tr}\exp(-\mathcal{H}/T)$ with E_i being the i th eigenvalue of \mathcal{H} , and $V_{i \rightarrow j}$ is the thermal jump matrix whose element at the j th row and i th column is one or zero in the energy representation. $V_{i \rightarrow j}$ fulfills $\beta_i \rho_E V_{i \rightarrow j} = \beta_j V_{i \rightarrow j} \rho_E$ with the equilibrium density matrix operator $\rho_E \equiv \exp(-\mathcal{H}/T)/\text{Tr}\exp(-\mathcal{H}/T)$ whose eigenvalues are β_i . This can be regarded as a detailed balance condition in equilibrium. The Lindblad equation (1) is a real-time dynamical equation which integrates both the quantum and the thermal contributions. It has been widely used in quantum optics [29] and relaxation processes in open quantum systems [27, 30]. Although for large couplings, Eq.(1) may be inapplicable [31], this equation gives a reasonable description in the weak coupling limit, for instance, for the time-independent \mathcal{H} , the steady solution of Eq. (1) is ρ_E independent of c [26–28], this is consistent with the foundation of statistical mechanics [32]. In the following, we focus on the weak coupling limit and consider the scaling properties of the Lindblad equation.

The theory of FTS [25] takes explicitly into account the rate R , which plays a role similar to L^{-1} since it imposes on a system an additional time scale that manipulates its evolution. In classical critical dynamics, the nonequilibrium dynamic scaling can be generalized directly from the equilibrium ones as confirmed by the renormalization-group theory [25]. However, in the nonequilibrium quantum criticality, as pointed out, a coupling strength must be considered as an independent scaling variable. In the weak coupling limit, this strength can be reduced to the dissipation rate c . Accordingly, for a length rescaling of factor b , an order parameter M transforms as

$$M(t, g, h_z, T, L, c, R) = b^{-\beta/\nu} M(tb^{-z}, gb^{1/\nu}, h_z b^{\beta\delta/\nu}, Tb^z, L^{-1}b, cb^z, Rb^r), \quad (2)$$

where the two critical exponents β and δ are defined as usual in classical critical phenomena by $M \propto g^\beta$ in the absence of an external probe field h_z conjugate to M and $M \propto h_z^\delta$ at $g = 0$, respectively. In the weak coupling limit, c is small thus one can expect its scaling behavior is controlled by the fixed point corresponding to the critical point at $c = 0$, thus the dimension of c is identical with t^{-1} as can be inspected from Eq. (1) [28]. This is checked latter by the numerical solution of Eq. (1).

With Eq. (2), one can describe in a unified framework different kinds of driven dynamics via changing g , h_z or T and readily define different regimes and their crossovers. Taking $g = Rt$ for instance, neglecting h_z , suppressing one independent variable, and choosing b such that Rb^r becomes a constant, one finds an FTS scaling form

$$M(g, T, L, c, R) = R^{\beta/\nu r} f_1(gR^{-1/\nu r}, TR^{-z/r}, L^{-1}R^{-1/r}, cR^{-z/r}), \quad (3)$$

where $r = z + 1/\nu$ obtained from $g = Rt$ and its rescaling [25] and the function f_i with an integer i denotes a scaling function. FTS dominates when $|g|R^{-1/\nu r} \ll 1$, $TR^{-z/r} \ll 1$, $L^{-1}R^{-1/r} \ll 1$, and $cR^{-z/r} \ll 1$. The first gives $\tau_d \sim R^{-z/r} \ll |g|^{-\nu z} \sim \tau_s$, the second $\tau_d \ll 1/T = \tau_T$ as they ought to be. Crossovers to other regimes occur near $|\hat{g}| \sim R^{1/\nu r}$ and $\hat{T} \sim R^{z/r}$ as depicted in Fig. 1 and similar ones for L and c . The first gives $|\hat{t}| \sim R^{-\nu z/(1+\nu z)}$ because $\hat{g} = R\hat{t}$. This is just the scaling of the KZM upon identifying \hat{t} with the freeze-out time instant [4, 5, 10] for a closed system $c = 0$ in the thermodynamic limit ($L \rightarrow \infty$) and at $T = 0$.

Several remarks are in order here. (a) Equation (3) is different from the similar scaling form for finite temperatures in [20] because c must be included to introduce the thermal fluctuation in the nonequilibrium situation. (b) To return to the equilibrium scaling form at finite-temperatures [1], the scaling function f_i must satisfy a constraint of $\partial f_i/\partial c = 0$ for $R = 0$. (c) Beside recovering the full scaling forms of finite-size for closed system in [13, 14] by fixing $c = 0$ and $T = 0$, the nonequilibrium dissipation scaling for spontaneous emissions in zero-temperature open quantum systems can also be studied by fixing $T = 0$ in Eq. (3). (d) Note that c should be small in the weak coupling limit and thus the regime dominated by c may be inaccessible.

Instead of sweeping g , when $h_z = R_z t$, one obtains similarly the order parameter

$$M_h = R_z^{\beta/\nu r_z} f_2(gR_z^{-1/\nu r_z}, h_z R_z^{-\beta\delta/\nu r_z}, TR_z^{-z/r_z}, L^{-1}R_z^{-1/r_z}, cR^{-z/r_z}) \quad (4)$$

with $r_z = z + \beta\delta/\nu$. Different regimes and their crossovers can also be readily defined. Different from sweeping g through the critical point as the ordinary KZM protocols [12–14, 20], here we fix g and change the symmetry breaking field h_z . This provides a method to determine the critical point from distinct critical behaviors for $g = 0$ and $g \neq 0$, a method which we shall utilize below and may also be realizable experimentally. Note that in this protocol, the form of τ_d remains remarkably if R and r are replaced with their counterparts. However, in addition to the fixed τ_s for the fixed g , there exists another reaction time diverging with $|h_z|^{-\nu z/\beta\delta}$. These result in new competitions but act only as corrections in the FTS regime, showing an advantage of FTS.

Now we show that FTS can provide methods to detect quantum critical properties such as the critical point and critical exponents. For simplicity, we consider $T = 0$ and $c = 0$ in the thermodynamic limit $L \rightarrow \infty$. According to Eq. (4), at $h_z = 0$, M_h reduces to

$$M_0(g, R_z) = R_z^{\beta/\nu r_z} f_3(gR_z^{-1/\nu r_z}), \quad (5)$$

while the field at $M_h = 0$, denoted by h_{z0} , scales as

$$h_{z0}(g, R_z) = R_z^{\beta\delta/\nu r_z} f_4(gR_z^{-1/\nu r_z}). \quad (6)$$

Differentiating M_h with respect to h_z in Eq. (4), one obtains the susceptibility at zero field,

$$\chi(g, R_z) = R_z^{\beta(1-\delta)/\nu r_z} f_5(gR_z^{-1/\nu r_z}). \quad (7)$$

To fix the critical point, we can define a cumulant

$$C(g, R_z) \equiv M_0/(h_{z0}\chi) = f_6(gR_z^{-1/\nu r_z}) \quad (8)$$

similar to the Binder cumulant in finite-size scaling [11]. As C is a function of only one independent variable, its curves for different R_z intersect at the critical point $g = 0$ at which C becomes a constant $f_6(0)$ independent on R_z . This gives the critical point with which all the critical exponents can then be estimated. For example, $\beta/\nu r_z$ and $\beta\delta/\nu r_z$ can be estimated respectively from Eqs. (5) and (6) by fitting M_0 and h_{z0} for a series of R_z at $g = 0$. Similarly, from Eq. (3) at $c = 0$, $T = 0$, and $L \rightarrow \infty$, $\beta/\nu r$ can be estimated by fitting M for a series of R at $g = 0$. From these three exponent ratios and the scaling law [1] $\beta(\delta + 1) = (d + z)\nu$ with the space dimensionality d , one can determine all the critical exponents.

As an example of the FTS method to determine critical properties, we consider the one-dimensional (1D) transverse-field Ising model whose Hamiltonian is [1]

$$\mathcal{H} = -h_x \sum_{n=1}^N \sigma_n^x - \sum_{n=1}^{N-1} \sigma_n^z \sigma_{n+1}^z, \quad (9)$$

and has been realized in CoNb₂O₆ experimentally [33], where σ_n^x and σ_n^z are the Pauli matrices, h_x is the transverse field, and the Ising coupling has been set to unity as our energy unit. The model exhibits a continuous QPT from a ferromagnetic phase to a quantum paramagnetic phase at a critical point h_{xc} (and so $g = h_x - h_{xc}$) at $T = 0$ [1]. The order parameter is the magnetization $M = \sum_{n=1}^N \langle \sigma_n^z \rangle / N$ for the N spins with the angle brackets denoting the quantum and/or thermal average. As a method to probe the transition, we add to \mathcal{H} a symmetry-breaking term $-h_z \sum_{n=1}^N \sigma_n^z$.

We illustrate our approach at $T = 0$ and $c = 0$ at which Eq. (1) is same to Schrödinger's equation and some exact results are available for comparison. We solve the model using the time-evolving block-decimation algorithm [34], which is capable of treating large system sizes. We determine the critical point in Fig. 2 and apply it purposely

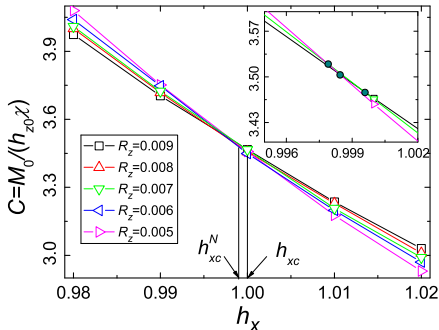


FIG. 2: (color online) Estimation of quantum critical point. Curves of the cumulant C for different R_z intersect at the critical point h_{xc} or $g = 0$. Owing to possible errors from the truncation of the singular values in the Schmidt decomposition [34], however, the intersections are slightly scattered as shown in the inset. Nevertheless, the average of all the intersections is $h_{xc}^N = 0.999(2)$, a good estimate of the exact value $h_{xc} = 1$. We choose a lattice size of $L = 2000$, which has been checked to produce a negligible size effect.

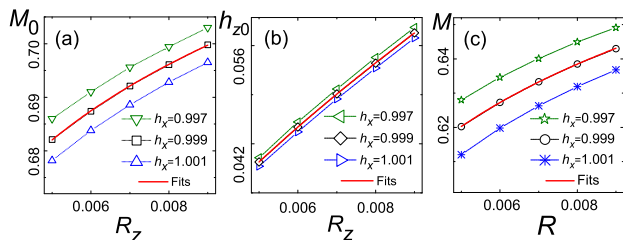


FIG. 3: (color online) Estimation of critical exponents. Our solutions with $h_{xc}^N = 0.999$, $T = 0$, and $L = 2000$ yield $\beta/\nu r_z = 0.0436$, $\beta\delta/\nu r_z = 0.651$, and $\beta/\nu r = 0.0622$ from power-law fits according to the scaling forms (5), (6) and (3), respectively. We then obtain all the critical exponents listed in Table I with their exact results for comparison. As the statistical errors of the fits are tiny, we fit data at $h_{xc} = 0.997$ and 1.001 and the largest difference in each exponent is used as an estimate of the error given also in Table I.

to determine the critical exponents in Fig. 3. The good agreement of the results collected in Table I shows the power of FTS.

Having successfully demonstrated FTS at $T = 0$, we now turn to $T \neq 0$ at which most experiments operate. To examine the general nonequilibrium FTS (4) for $T \neq 0$, we solve numerically Eq. (1) for the Hamiltonian (9) along with the field h_z by a finite difference method to second order with periodic boundary conditions. We find that M_h can now saturate correctly with the thermal fluctuations. Moreover, Fig. 4 shows clearly the validity of the FTS form (4). Further, upon comparing (a) with (b) in Fig. 4, it is obvious that c must enter

TABLE I: Critical point and exponents for the 1D transverse-field Ising model

	h_{xc}	β	δ	ν	z
Numerical	0.999(2)	0.125(11)	14.9(6)	0.98(4)	1.01(3)
Exact [1]	1	0.125	15	1	1

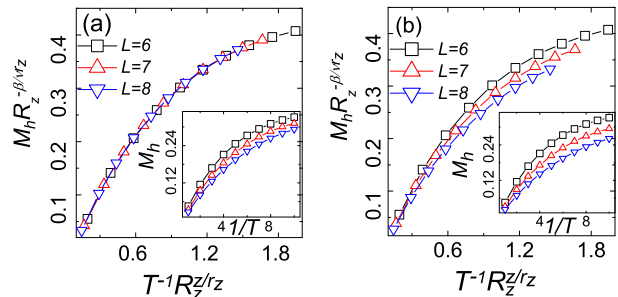


FIG. 4: (color online) Nonequilibrium scaling at nonzero temperatures. (a) Data of M_h versus T plotted in the inset for the three different sets of R_z , c , and L so choosing as to fix the value of $L^{-1}R_z^{-1/r_z}$ and cR_z^{-z/r_z} collapse as expected onto a single curve for the fixed $LR_z^{1/r_z} = 1.166$ and $cR_z^{-z/r_z} = 3.603$ according to the FTS (4) at $g = 0$ ($h_x = 0.999$), $h_z = 0$. (b) If, instead of cR_z^{-z/r_z} , we fix all $c = 0.7$, the value for $L = 6$, and keep others, the rescaled curves then do *not* collapse.

into the scaling forms with a scaling dimension z . Note that although here we only solve directly Eq. (1) for small lattices, the results show that it is suitable for describing the nonequilibrium behavior at finite temperatures near the quantum critical point. Moreover, the rapidly developing numerical renormalization-group methods [35], for example, seem quite promising to solve the equation for larger lattice sizes [36].

In conclusion, FTS not only provides a unified understanding of the driving dynamics in general and lights up the dark impulse regime of KZM at zero temperature in particular, but also sheds light on the QCR at nonzero temperatures by establishing its own regime. It offers a powerful unified approach amenable to both numerics and experiments to study equilibrium and nonequilibrium dynamics of quantum criticality. We have shown that in the latter in open systems one must include the dissipation rate as an independent scaling variable and the Lindblad equation can be a valuable framework for such studies. Although we have studied a simple model for illustration, our approach should be applicable to more complex systems as well. In addition, as our results indicate that the classical theory of FTS with proper modifications can well describe quantum criticality, new physics may be in action [2] if it is violated.

We thank Junhong An, Peter Drummond, and

Xiwen Guan for their valuable comments and discussions. Y.S. and F.Z. were supported by NNSFC (10625420) and FRFCUC. C.L. was supported by NNSFC (11075223), NBRPC (2012CB821300 (2012CB821305)), NCETPC (NCET-10-0850). We acknowledge use of some source codes for TEBD from <http://physics.mines.edu/downloads/software/tebd/>.

* Electronic address: zsuynshuai@163.com

† Electronic address: lichaoh2@mail.sysu.edu.cn

‡ Electronic address: stszf@mail.sysu.edu.cn

- [1] S. Sachdev, *Quantum Phase Transitions*, (Cambridge University Press, 1999).
- [2] P. Coleman and A. J. Schofield, *Nature* **433**, 226 (2005).
- [3] S. Sachdev and B. Keimer, *Phys. Today* **64**(2), 29 (2011).
- [4] J. Dziarmaga, *Adv. Phys.* **59**, 1063 (2010).
- [5] A. Polkovnikov, K. Sengupta, A. Silva, and M. Vengalattore, *Rev. Mod. Phys.* **83**, 863 (2011).
- [6] M. Greiner, *et al.*, *Nature* **415**, 39 (2002).
- [7] X. Zhang, C-L. Hung, S-K. Tung, and C. Chin, *Science* **335**, 1070 (2012).
- [8] T. Kibble, *J. Phys. A: Math. Gen.* **9**, 1387 (1976); *Phys. Today* **60**(9), 47 (2007).
- [9] W. H. Zurek, *Nature* **317**, 505 (1985).
- [10] W. H. Zurek, U. Dorner, and P. Zoller, *Phys. Rev. Lett.* **95**, 105701 (2005); J. Dziarmaga, *Phys. Rev. Lett.* **95**, 245701 (2005); A. Polkovnikov, *Phys. Rev. B* **72**, 161201(R) (2005); B. Damski and W. H. Zurek, *Phys. Rev. Lett.* **99**, 130402 (2007); F. M. Cucchietti, B. Damski, J. Dziarmaga, and W. H. Zurek, *Phys. Rev. A* **75**, 023603 (2007); L. Cincio, J. Dziarmaga, M. M. Rams, and W. H. Zurek, *Phys. Rev. A* **75**, 052321 (2007); V. Mukherjee, U. Divakaran, A. Dutta, and D. Sen, *Phys. Rev. B* **76**, 174303 (2007); D. Sen, K. Sengupta, and S. Mondal, *Phys. Rev. Lett.* **101**, 016806 (2008); S. Mondal, K. Sengupta, and D. Sen, *Phys. Rev. B* **79**, 045128 (2009); C. Lee, *Phys. Rev. Lett.* **102**, 070401 (2009); C. De Grandi, V. Gritsev, and A. Polkovnikov, *Phys. Rev. B* **81**, 012303 (2010); C. De Grandi, V. Gritsev, and A. Polkovnikov, *Phys. Rev. B* **81**, 224301 (2010).
- [11] D. P. Landau and K. Binder, *A Guide to Monte Carlo Simulations in Statistical Physics*, 2nd edition (Cambridge University Press, Cambridge, 2009).
- [12] S. Deng, G. Ortiz, and L. Viola, *Europhys. Lett.* **84**, 67008 (2008).
- [13] C. De Grandi, A. Polkovnikov, and A. W. Sandvik, *Phys. Rev. B* **84**, 224303 (2011).
- [14] M. Kolodrubetz, D. Pekker, B. K. Clark, and K. Sengupta, *Phys. Rev. B* **85**, 100505(R) (2012); M. Kolodrubetz, B. K. Clark, and D. A. Huse, *Phys. Rev. Lett.* **109**, 015701 (2012).
- [15] G. Biroli, L. F. Cugliandolo, and A. Sicilia, *Phys. Rev. E* **81**, 050101(R) (2010); A. Jelic and L. F. Cugliandolo, *J. Stat. Mech.* P02032 (2011).
- [16] A. Polkovnikov and V. Gritsev, *Nat. Phys.* **4**, 477 (2008); S. Sotiriadis, P. Calabrese, and J. Cardy, *Europhys. Lett.* **87**, 20002 (2009). V. Gritsev and A. Polkovnikov, in *Understanding Quantum Phase Transitions*. ed. L. D. Carr, (Taylor & Francis, Boca Raton, 2010); S. Deng, G. Ortiz, and L. Viola, *Phys. Rev. B* **83**, 094304 (2011).
- [17] S. Chakravarty, B. I. Halperin, and D. R. Nelson, *Phys. Rev. B* **39**, 2344 (1989).
- [18] D. M. Broun, *Nat. Phys.* **4**, 170 (2008).
- [19] D. Patanè, A. Silva, L. Amico, R. Fazio, and G. E. Santoro, *Phys. Rev. Lett.* **101**, 175701 (2008).
- [20] A. Chandran, A. Erez, S. S. Gubser, and S. L. Sondhi, *Phys. Rev. B* **86**, 064304 (2012).
- [21] We thank an anonymous referee for pointing out this to us.
- [22] T. Kinoshita, T. Wenger, and D. S. Weiss. *Nature* **440**, 900 (2006).
- [23] S. Hofferberth, *et al.*, *Nature* **449**, 324 (2007).
- [24] M. Rigol, V. Dunjko, and M. Olshanii, *Nature* **452**, 854 (2008).
- [25] S. Gong, F. Zhong, X. Huang, and S. Fan, *New J. Phys.* **12**, 043036 (2010); F. Zhong, in *Applications of Monte Carlo Method in Science and Engineering*. ed. S. Mordechai, p469 (Intech, 2011). Available at <http://www.intechopen.com/books/applications-of-monte-carlo-methods>
- [26] G. Lindblad, *Commun. Math. Phys.* **48**, 119 (1976).
- [27] S. Attal and A. Joye, *J. Func. Analysis.* **247**, 253 (2007).
- [28] P. Mai, Derivation of the Lindblad equation from a microscopic mechanism in which the open Ising chain coupling weakly with an infinite thermal bath. (unpublished).
- [29] M. Orszag, *Quantum optics*, 2nd Edition. (Springer, 2008).
- [30] M. Žnidarič, T. Prosen, G. Benenti, G. Casati, and D. Rossini, *Phys. Rev. E* **81**, 051135 (2010).
- [31] W. G. Wang, *Phys. Rev. E* **86**, 011115 (2012).
- [32] E. Schrödinger, *Statistical Thermodynamics* (Cambridge University Press, Cambridge, England, 1952); S. Goldstein, J. L. Lebowitz, R. Tumulka, and N. Zanghi, *Phys. Rev. Lett.* **96**, 050403 (2006); J. Cho and M. S. Kim, *Phys. Rev. Lett.* **104**, 170402 (2010); S. Goldstein, *et al.*, *Phys. Rev. E* **81**, 011109 (2010); S. Popescu, A. J. Short, and A. Winter, *Nature Phys.* **2**, 754 (2006).
- [33] R. Coldea, *et al.* *Science* **327**, 177 (2010).
- [34] G. Vidal, *Phys. Rev. Lett.* **93**, 040502 (2004).
- [35] F. Verstraete, V. Murg, and J. I. Cirac, *Adv. Phys.* **57**, 143 (2010).
- [36] F. Verstraete, J. J. García-Ripoll, and J. I. Cirac, *Phys. Rev. Lett.* **93**, 207204 (2004); M. Zwolak and G. Vidal, *Phys. Rev. Lett.* **93**, 207205 (2004).